IOP Conference Series: Materials Science and Engineering

PAPER • OPEN ACCESS

Metal Foam-Filled Tubes as Plastic Dissipaters in Earthquake-Resistant Steel Buildings

To cite this article: C Ghiani *et al* 2018 *IOP Conf. Ser.: Mater. Sci. Eng.* **416** 012051

Metal Foam-Filled Tubes as Plastic Dissipaters in Earthquake-Resistant Steel Buildings

C Ghiani[1], E Linul[2,*], MC Porcu[1], L Marsavina[2], N Movahedi[3] and F Aymerich[1]

[1]Department of Mechanical, Chemical and Materials Engineering, University of Cagliari, via Marengo 2, Cagliari, Italy
[2]Department of Mechanics and Strength of Materials, Politechnica University of Timisoara, 1 Mihai Viteazu Avenue, 300 222 Timisoara, Romania
[3]Independent Researcher (Graduated from Semnan University), Isfahan, Iran

[*]Corresponding author: emanoil.linul@upt.ro

Abstract. The aim of this paper is to investigate whether metal-foam-made devices can be effective to dissipate seismic energy in buildings during strong earthquakes. To this purpose, non-linear numerical analyses of concentrically braced steel buildings under recorded ground motions have been carried out, while some experimental tests on metal-foam specimens and metal-foam-filled tubes have been performed. Foam-based devices are assumed to be inserted within the diagonal braces of the considered steel frame to dissipate energy by plastic deformation during strong earthquakes. To apply the experimental data, a scaled numerical model of the prototype building has been implemented by means of the similitude theory and the Buckingham Π theorem. The results of the study provide a preliminary assessment of the potential of metal foam-based dissipaters to reduce the seismic effects in civil structures.

1. Introduction

Metal foams are a relatively novel class of materials used for several applications mostly in the mechanical engineering field [1-3]. Among their high-performance properties are weight-to-stiffness ratio, damping and energy dissipation, thermal resistivity and acoustic absorption [4, 5]. In particular, owing to their excellent energy absorption characteristics, metal foams are widely used in the mechanical, aerospace and automotive applications, as, for instance, shock mitigation in vehicles, cf. e.g. [6]. On the contrary, they are still scarcely used in civil engineering, as addressed in [7]. However, the capability to dissipate energy that metal foams typically possess could be exploited to control the seismic effects on buildings.

Different strategies are actually adopted to reduce the seismic stress on civil structures during exceptional events. Typically they are based on (i) the ductile behavior of structural elements or connections, [8], (ii) base-isolation [9] or mass reduction [10] techniques, (iii) dampers or dissipaters introduced in the structure [11]. The feasibility of using metallic foams to dissipate seismic energy in concentrically-braced (CB) steel buildings was firstly explored in [12] while the effectiveness of filling tubular steel elements with metallic foams to increase their ductility and bucking resistance was shown in [13]. Although CB frames may perform very well under seismic actions, cf. [14], diagonal braces were found to experience perform severe concentration of plastic-deformation in their mid-length section, which may lead to premature brace fracture and frame failure [15]. For this reason modified or hybrid diagonal braces were proposed [12, 15].

The present paper aims to further investigate on the possible application of metallic foams (MFs) and foam-filled tubes (FFTs) within the diagonal braces of CB steel frames to dissipate large amount of energy during severe earthquakes. The results of some experimental tests were exploited to obtain an idealized elastic-plastic behavior of foam-based devices to be implemented in the numerical model. Non-linear dynamic numerical analyses were carried out on full-scale and scaled models of a case-study steel building with and without metal-foam-based devices. The results leaded to evaluate the percentage of stress reduction achievable under real ground motions. This study is just a preliminary phase of a wider investigation involving cyclic tests on foams and foam filled tubes, as well as several parametric non-linear analyses on different steel structures under many severe earthquakes.

2. Experimental tests on metallic foams and foam-filled tubes

Closed-cell metallic (aluminum alloy) foams (Fig. 1a) with two different densities (420 kg/m^3 and 750 kg/m^3) were manufactured by casting technique. All details about aluminum alloy foams preparation has been described in Ref. [16]. The cylindrical specimens (height = 20 mm, diameter = 20 mm) were cut from large foam blocks using Electric Discharge Machining. The obtained specimens were tested both separately (only foam) [17] and as core material in cylindrical thin-walled (1 mm thickness) 304 stainless steel tubes (see Fig. 1b) [18, 19]. Quasi-static uniaxial compression tests were carried out at room temperature on a 100 kN LBG testing machine (see Fig. 1c), with a constant crosshead speed of 10 mm/min, according to the ISO13314-11 standard [20].

The stress-strain diagrams obtained for 420-MF (420 kg/m^3 foam density), 750-MF (750 kg/m^3 foam density) and 420-FFT (750 kg/m^3 foam-filled tube) specimens under quasi-static compression tests are provided in Fig. 2. The behavior obtained in this case is typical to other closed-cell metallic foams and advanced composite foam structures, highlighting three very important regions in the field of energy absorption: linear-elastic, plateau and densification regions [21, 22].

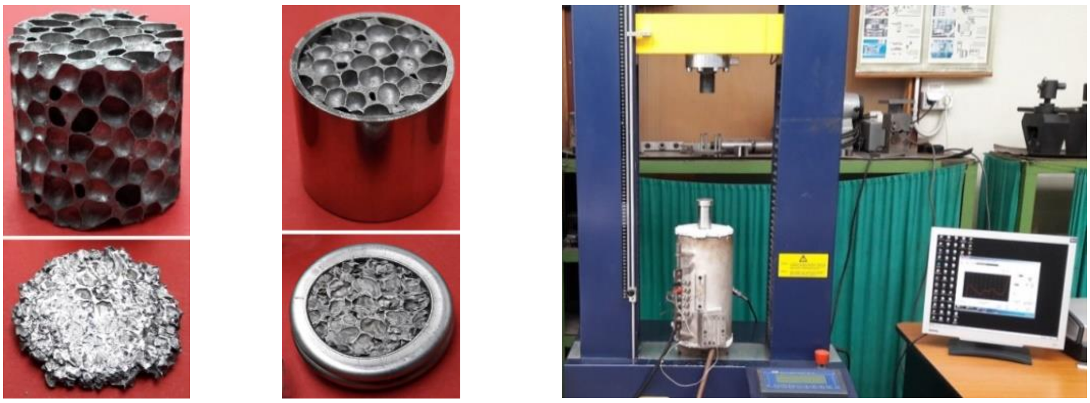

(a) MF specimen (b) FFT specimen (c) The 100 kN LBG quasi-static testing machine

Figure 1. The specimens before and after the loading (a, b), and experimental test set-up (c)

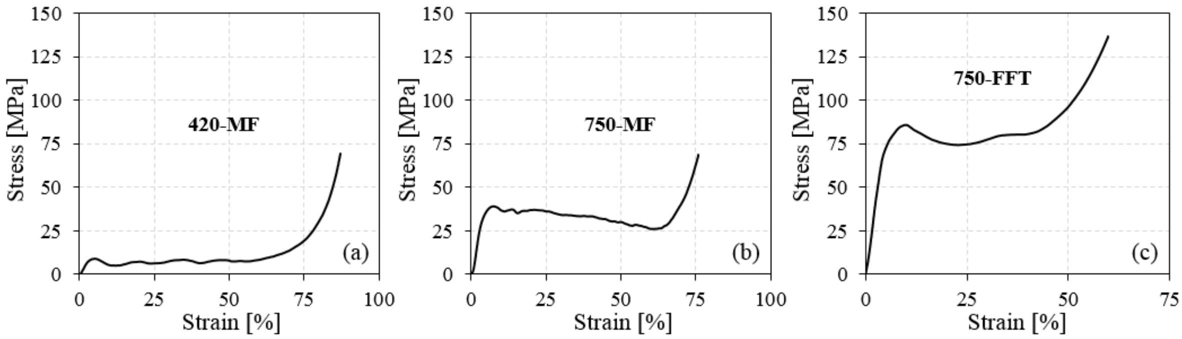

Figure 2. Stress-strain curves of (a) 420 kg/m3 metal foam (420-MF); (b) 750 kg/m3 metal foam (750-MF) and (c) foam-filled-tube (750-FFT) under quasi-static compression loading.

The results of the experimental tests evidenced a remarkable ductile and dissipative behavior of both MFs and FFTs under compression loads. A comparison between the diagrams in Fig. 2 evidences that the yield stress may range from values lower than 10 MPa to values greater than 100 MPa depending on the foam density and on the properties of tubes. In particular, changing the thickness of the tube or lightening the tube wall may result in lowering the yield stress of FFTs.

It is to note, however, that the experimental results presented in this section may give just a coarse idea of the behavior of MFs and of FFTs under seismic actions. Further tests should, in fact, be performed to obtain the hysteretic behavior of MFs and FFTs (accounting for stiffness and/or strength degradation) under cyclic loads.

3. Numerical model of a braced steel frame with metal-foam-based dissipaters

A four-story inverted V bracing framed steel building was considered, making reference to [14]. Some geometrical details of the building are provided in Fig.3. In Table 1 are given the static loads calculated according to Eurocode 1 [23], while Table 2 lists the cross section types of the steel elements. A 3D model of the building was implemented with the finite element program SAP2000 [24]. Columns and beams were modelled through elastic straight frame elements. Fixed beam to column connections and fixed constraints to the ground were assumed. Rigid diaphragms were considered at the floor slabs. Diagonal braces were modelled as capable to resist only axial actions (truss elements). A cylindrical MF dissipater was supposed to be inserted in the mid of each diagonal brace, as drafted in Fig. 3. The MF plastic dissipater was modelled through a 1-degree of freedom (longitudinal) plastic hinge with kinematic hardening unloading. Calculated according to EC8 [25], lumped masses are considered acting at the building floors. A damping ratio of 5%, which is a common value for steel structures was assumed. Time-history non-linear analyses were carried out under a strong recorded earthquake, see Fig. 3d, supposed to be applied both in the x and y directions.

Table 1. Static loads

Dead loads	Live loads	Wind load
4.44 kN/ m^2	2.00 kN/m^2	0.49 kN/m^2

Table 2. Cross section types

Columns	Beams	Diagonal braces
W14x211	W14x48	PIPE8XXS

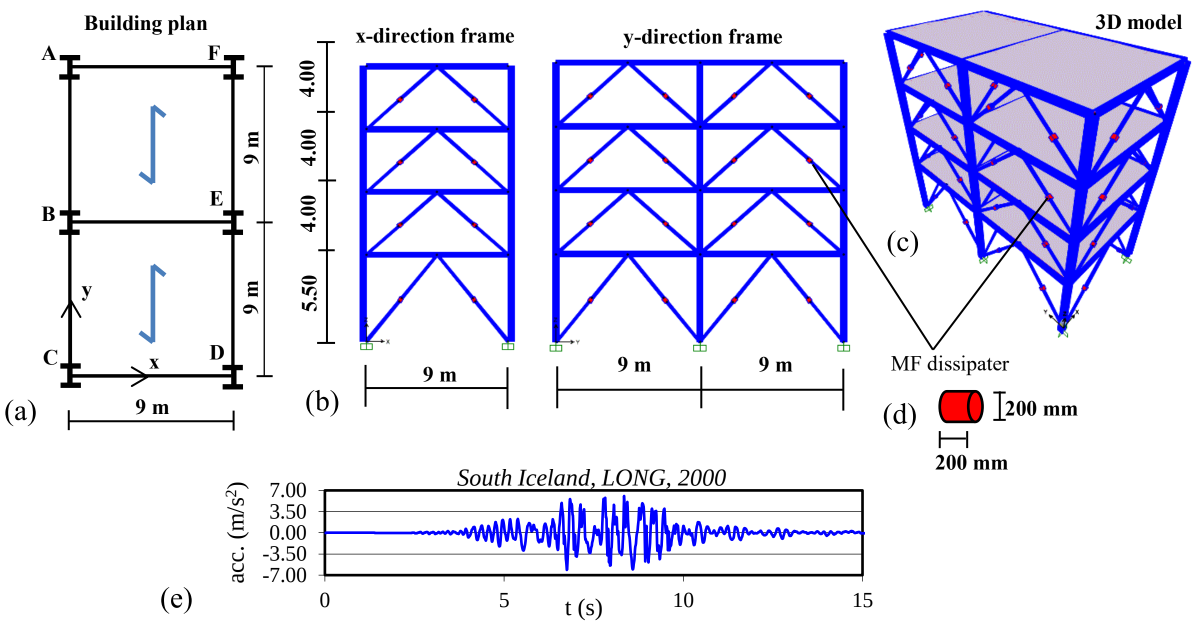

Figure 3. Case-study building. (a) Building plan; (b) frames in the x and y direction; (c) 3D model; (d) size of the MF dissipater; (e) South Iceland 2000 earthquake.

The experimental data provided in Section 2 can be exploited to calibrate the behavior of the foam-based devices to be introduced within the numerical model, as discussed in Section 3.1. Due to the small-size of the cylindrical specimens tested (20 mm diameter and height), however, the numerical investigation should be performed on a scaled model of the prototype building of Fig.1. Based on a dimensional analysis, the procedure to obtain a scaled model is presented in Section 3.2.

3.1. MF plastic dissipaters

Although exhibiting a remarkable ductile behavior under compressive loading, foams typically have a very low resistance under tension loading. Of course, the tension strength may be strongly increased if foam-filled tubes are considered instead of bare foams. For a preliminary concept analysis, however, MF dissipaters are here assumed to be made by bare foam and to resist only to compression.

To size the MF device, the following equation can be used:

$$\sigma_y = \frac{4F_y}{\pi D_f^2} \tag{1}$$

where F_y denotes the axial yielding load value for the MF dissipater. By assuming that any building member (even the MF dissipaters) should resist static and wind loads by deforming in the elastic range, the value of F_y can be derived from a linear static analysis. As derived from it, the value $F_y = 400\ kN$ is thus set for the present case-study. By assuming that the diameter of the cylindrical MF device is almost equal to the outer diameter of the tubular braces (PIPE8XXS), that is $D_f = 200\ mm$, the following yield stress for the foam device should be considered: $\sigma_y \cong 12.50\ MPa$.

The idealized bilinear stress-strain curve plotted in black in Fig. 4a was thus assumed in the present investigation. As can be inferred form Fig.4a, the idealized curve is slightly higher than the experimental one relevant to the 420-MF specimen. The force-displacement curve implemented in SAP2000 to represent the behavior of the MF device is given in Fig. 4b. Conventionally, compression stress and strain have negative sign for SAP2000. Since MF devices can only withstand compression loads, the diagonal braces are expected to work alternately during an earthquake. This assumption is rather strong and imply a detailed design of the MF devices for practical applications. Should FFT devices be considered instead, a tension-compression constitutive behavior could be considered.

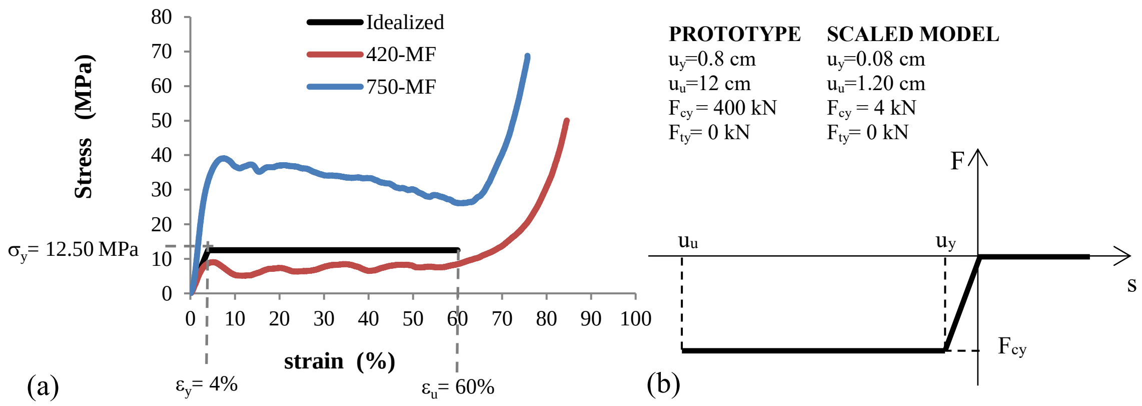

Figure 4. (a) Idealized bilinear constitutive stress-strain curve of MF dissipaters; (b) force-displacement curve of the MF dissipater as implemented in SAP2000.

The yield and failure values of force and displacement adopted for the MF devices are provided in Fig.4b. To avoid buckling of the hybrid brace (consisting of two equal steel tubes with a central cylindrical MF device) the critical load P_{cr} should be larger than the yield compression load F_{cy}. By considering the hybrid brace as a stepped column, the value of P_{cr} can be obtained by solving the following transcendental equation with a trial-and-error method [26]:

$$tan\left[L_s\left(\frac{P_{cr}}{E_sI_s}\right)^{1/2}\right]tan\left[L_f\left(\frac{P_{cr}}{E_fI_f}\right)^{1/2}\right]=\left(\frac{E_f\,I_f}{E_s\,I_s}\right)^2 \qquad (2)$$

Here E_s and E_f are the elastic moduli while I_s and I_f are the inertia moments of steel and foam cross sections, respectively. In the present case, $E_s = 199948\ MPa$, $E_f = 312.50\ MPa$, $I_s = 1.227\ mm^4$ and $I_f = 0.991\ mm^4$. Due to symmetry with respect to the mid-section, it can be put $L_s = L/2$ and $L_f = a/2$, being L the length of the hybrid element and a the length of the MF device (here $L_s = 3569\ mm$ and $L_f = 100\ mm$). The value $P_{cr} = 806.19\ kN > F_{cy}$ was thus finally obtained.

Since, however, the diameter of the MF dissipaters ($D_f = 200\ mm$) to be introduced in the full-scale building (prototype) is about ten times greater than the diameter of the specimens tested in laboratory ($20\ mm$) [27], a scaled model should be introduced in the numerical investigation, as discussed in the next section.

3.2. Scaled model of the steel building

To exploit experimental results in the numerical investigation, a scaled model was considered in the present study. This is a rather usual approach in Civil Engineering, due to the very large dimensions of the full-scale models, see e.g. [28, 29]. The stress σ in a point of interest is chosen as the dependent variable giving the seismic response of the steel building and assumed to be function of 6 independent parameters: time (t), density of materials (ρ), elastic properties of materials (E), ground acceleration (a), gravity acceleration (g) and all geometric dimensions (L). That is:

$$\sigma = f(\ t,\ \rho,\ E,\ a_g,\ g,\ L\ ) \qquad (3)$$

The fundamental dimensions of the mechanical problem being three, according to Buckingham's Π theorem, the number of independent dimensionless π-parameters is (6-3)=3. Eq. (1) then becomes:

$$\frac{\sigma}{E} = g\left(\frac{t}{L}\sqrt{\frac{E}{\rho}}\ ,\ \frac{a}{g}\ ,\ \frac{gL\rho}{E}\right) \qquad (4)$$

with

$$\Pi_1 = \frac{\sigma}{E}\ ,\quad \Pi_2 = \frac{t}{L}\sqrt{\frac{E}{\rho}}\ ,\ \Pi_3 = \frac{a}{g}\ ,\quad \Pi_4 = \frac{gL\rho}{E}\ , \qquad (5)$$

Owing to the fact that the gravity acceleration cannot be scaled (except for very specific test conditions), from equality $(\Pi_3)_p = (\Pi_3)_m$ (subscript p and m denoting quantity related to prototype and to scaled model, respectively) it is found that the scale factor for accelerations is $S_g = S_a = 1$. As a consequence, from equality $(\Pi_4)_p = (\Pi_4)_m$ follows that $S_E/S_\rho = S_L$. As usually done in structural dimensional analysis, the same elastic modulus of the materials is assumed in the prototype and in the model, i.e. $S_E = 1$, which implies $S_\sigma = 1$ and $S_\rho = 1/S_L$. Table 3 summarizes the scale factors for the main physical variables of the considered problem. Aside from those equal to 1, all scale factors in Table 3 are function of the length scale factor S_L. In the present investigation we put $S_L = 10$. This value is given in fact by the ratio between the diameter of the foam devices to be inserted in the prototype (200 mm) and the diameter of the tested specimens (20 mm). When modelling the constitutive behavior of the MF device in the scaled model the values given in Fig.4b should be considered, as derived by the scaling procedure.

Table 3. Scale factors

physical variable	unit	Scale factor
Length (L)	mm	1: S_L
Area (A)	mm^2	1: S_L^2
Volume (V)	mm^3	1: S_L^3
Density (ρ)	kg/ mm^3	S_L:1
Mass (M= ρV)	kg	1: S_L^2
Time (t)	s	1:(S_L)$^{1/2}$
Frequency (f=1/t)	Hz	(S_L)$^{1/2}$:1
Acceleration (a)	mm/s^2	1:1
Force (F=Ma)	kN	1: S_L^2
Young's modulus (E)	kN/mm^2	1:1
Stress (σ)	kN/mm^2	1:1

4. Results of the numerical investigation

A full-scale model (prototype) and a scaled model of the case-study building were modelled with SAP2000. First, the case of a linear elastic model of the building without MF dissipaters was studied. Secondly, the non-linear MF dissipaters were introduced in both the prototype and the scaled models. The first five frequencies of the two models are compared in Table 4 for the two considered cases (with and without MF dissipaters). As expected, the frequencies of the non-linear model (with the MF dissipaters), which is a more flexible system, are smaller than those of the linear model. It can be also noted that the scale factor for frequency $S_f = \sqrt{S_L} \cong 3.16$ (see Table 3) is always fulfilled both for linear and nonlinear models. Therefore, a good accuracy of the prototype response prediction through the scaled model is expected to be found.

Table 4. First five numerical eigen-frequencies

	without MF dissipaters			with MF dissipaters		
Freq.	Prototype	Scaled-model	Scale factor	Prototype	Scaled-model	Scale factor
1	5.46 Hz	17.27 Hz	3.16:1	2.11 Hz	6.69 Hz	3.16:1
2	6.53 Hz	20.67 Hz	3.16:1	2.36 Hz	7.47 Hz	3.16:1
3	14.90 Hz	47.14 Hz	3.16:1	2.62 Hz	8.28 Hz	3.16:1
4	17.12Hz	54.16 Hz	3.16:1	6.41 Hz	20.30 Hz	3.16:1
5	23.80 Hz	75.27 Hz	3.16:1	7.03 Hz	22.24 Hz	3.16:1

Some of the results of the numerical investigation are provided in Figs. 5-7. The shear values $V_x(t)$ and $V_y(t)$ at the base of column B are compared in Fig.5 for the scaled model with and without MF devices. It is found that a stress reduction up to 50 % can be achieved. Very similar results were found for the other columns of the scaled model. The same reduction (in percent) was found also for the prototype. However, a reduction in stress can often be paid in terms of displacement demand. The diagrams of Fig. 6 highlight, in fact, that a larger interstorey drift is found in the building with MF dissipaters. However, the EC8 [25] limit value $d_{LIM} = 0.01h/v$ is not exceeded. For the prototype it is $d_{LIM} = 100\ mm$ ($h = 4\ m$ and the importance factor $v = 0.4$), while $d_{LIM} = 10\ mm$ for the scaled model. A residual (plastic) displacement in both directions is kept after the seismic excitation.

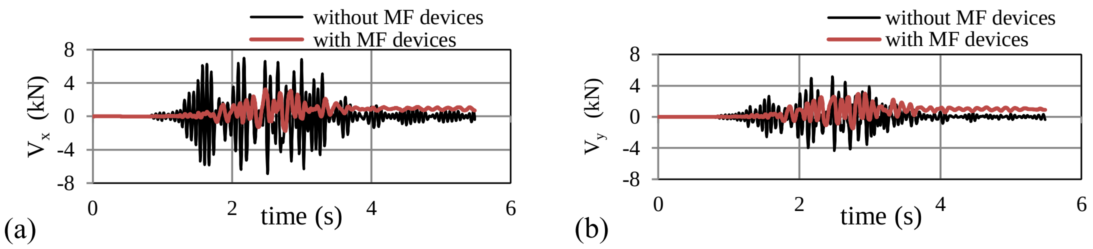

Figure 5. Scaled model. Column B base shear in (a) x-direction and (b) y-direction.

The hysteresis cycles of the MF dissipaters placed within two first story concentric braces are given in Fig. 7a while the corresponding axial loads are compared in Fig. 7b, showing that the expected alternate behavior is rightly exhibited by any couple of concentric diagonal braces.

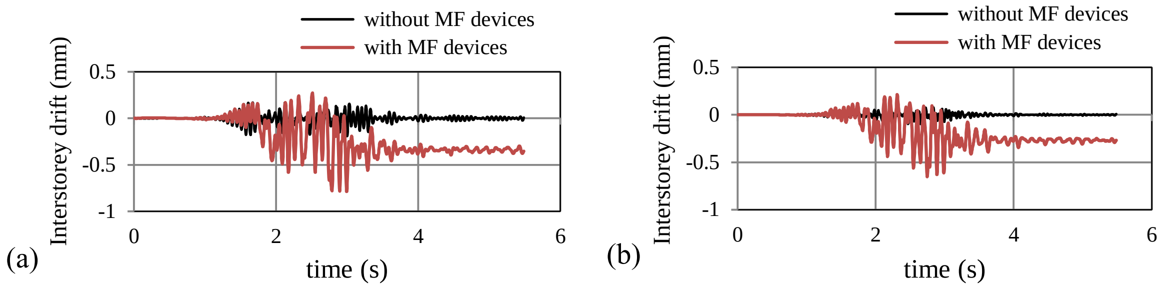

Figure 6. Interstorey drift at the upper storey in (a) x-direction and (b) y-direction

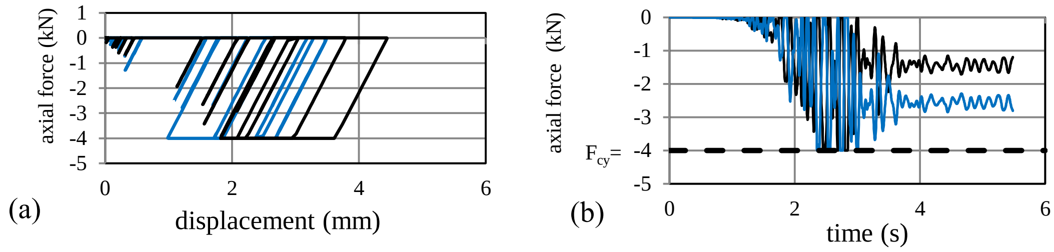

Figure 7. (a) Hysteresis cycles and (b) axial loads in the MF dissipaters of two opposite braces.

5. Conclusions

Similarly to other anti-seismic devices, also a foam-made dissipater is expected to behave like a mechanical fuse where damage concentrates under strong horizontal actions, one of the main advantages being that it can be dismounted and replaced after the seismic event. Of course, the practical design of foam-made devices entails different requirements also depending on whether bare foam devices or foam-filled tubes are considered and should be tuned according to the objectives of the seismic performance to be achieved by the building. One of the main concern of this work was to carry out a preliminary study on the effectiveness of MF dissipaters to reduce the seismic effects in buildings during severe earthquakes. To this purpose, a concept analysis was developed, based on some experimental data and involving linear and non-linear dynamic analyses of a 3D case-study steel building under a real ground motion. The experimental results and the numerical simulations on which the paper is based are just a preliminary stage of a wider investigation that will involve cyclic loading tests, full-scale specimens, suites of significant earthquakes and different building types.

6. References

[1] Simancik F, Degischer HP, Körner C, Singer et al. 2002 *Handbook of cellular metals: production, processing, applications*, Wiley, Weinheim
[2] Marsavina L, Kovacik J, Linul E 2016 *Theor. Appl. Fract. Mech.* **83** 11-18
[3] Linul E, Marsavina L, Kováčik J 2017 *Mat. Sci. Eng.-A Struct.* **690** 214-224
[4] Taherishargh M, Linul E, Broxtermann S, Fiedler T 2018 *J. Alloy. Compd.* **737** 590-596
[5] Kovácik J, Jerz J, Mináriková N et al. 2016 *Frattura ed Integrita Strutturale* **36** 55-62
[6] Duarte I, Vesenjak M, Krstulović-Opara L 2014 *Compos. Struct.* **109** 48-56
[7] Smith BH, Szyniszewski S et al. 2012 *J. Constr. Steel Res.* **71** 1-10
[8] Porcu MC 2017 Ductile Behavior of Timber Structures under Strong Dynamic Loads *Wood in Civil Engineering* Giovanna Concu (Ed.) InTech DOI: 10.5772/65894
[9] Kelly JM 1986 *Soil Dyn. Earthq. Eng.* **5(4)** 202-216

[10] Porcu MC 2013 *WIT Transactions on the Built Environment* **132**, 333-344
[11] Symans MD, Charney F A et al. 2008 *J. Struct. Eng.* **134(1)** 3-21
[12] Moradi M 2011 *Structural applications of metal foams considering material and geometrical uncertainty*, 37-88, PhD Thesis, University of Massachusetts Amherst.
[13] Moradi M and Arwade SR 2014 *Struct. Eng. Mech* **51(6)** 1017-1036
[14] Sabelli R, Mahin S, Chang C 2003 *Eng. Struct.* **25(5)** 655-666
[15] Vayas I (Ed) 2017 *Innovative anti-seismic devices and systems* The INNOSEIS Project RFCS-02-2015, pp. 1-423.
[16] Linul E, Movahedi N, Marsavina L 2018 *J. Alloy. Compd.* **740** 1172-1179
[17] Movahedi N, Linul E, Marsavina L 2018 *J. Mater. Eng. Perform.* **27(1)** 99-108
[18] Linul E, Movahedi N, Marsavina L 2017 *Compos. Struct.* **180** 709-722
[19] Movahedi N and Linul E 2017 *Mater. Lett.* **206** 182-184
[20] ISO13314-2011 Mechanical testing of metals-Ductility testing-Compression test for porous and cellular metals
[21] Linul E, Şerban DA, Marsavina L, Kovacik J 2017 *Fatigue & Fracture of Engineering Materials & Structures* **40(4)** 597-604
[22] Linul E, Marsavina L, Kovacik J, Sadowski T 2017 *P. Romanian Acad. A* **18(4)** 361-369
[23] EN, B. (1991). 1-2: 2002 *Eurocode 1: Actions on structures—Part 1-2: General actions—Actions on structures exposed to fire* British Standards
[24] CSI, SAP2000 rel.17 2014 *Integrated Finite Element Analysis and Design of Structures Basic Analysis Reference Manual* Computers and Structures Inc. Berkeley California USA
[25] CEN. 2004 *Eurocode 8: Design of Structures for Earthquake Resistance*, European Comitee for Standardization, Brussels, 1-232
[26] Timoshenko SP and Gere JM 1961 *Theory of elastic stability* McGrawHill-Kogakusha Ltd Tokyo
[27] Linul E, Movahedi N, Marsavina L 2018 *Materials* **11(4)** 554
[28] Stavridis A, Shing B, Conte J 2010 Design, Scaling, Similitude and Modeling of Shake-Table Test Structure, *Shake Table Training Workshop* San Diego
[29] Moncarz P and Krawinkler H 1981 *Theory and Application of Experimental Model Analysis in Earthquake Engineering* Rpt. No. 50 John Blume Earthquake Eng. Ctr. Stanford Univ.

Acknowledgments
This work was partially supported by research grants PCD-TC-2017 and by *Fondazione Sardegna* (University of Cagliari, Italy). The Visiting Professor Program of Regione Sardegna, the ERASMUS+STUDIO Program (ROTIMISOA04) and the MOSTA (Staff Mobility) Program of the University of Cagliari are also acknowledged.